

PERFORMANCE EVALUATION OF HL-LHC CRAB CAVITY PROTOTYPES IN A CERN VERTICAL TEST CRYOSTAT

K. G. Hernández-Chahín*, DCI-UG, Guanajuato, México,

A. Macpherson, C. Jarrige, M. Navarro-Tapia, R. Torres-Sánchez, CERN, Geneva, Switzerland,
G. Burt, A. Tutte, Cockcroft Institute, Cheshire, UK, S. Verdú-Andrés, BNL, Long Island, NY, US,
S. U. De Silva, ODU, VA, USA

Abstract

Three proof-of-principle compact crab cavity designs have been fabricated in bulk niobium and cold tested at their home labs, as a first validation step towards the High Luminosity LHC project. As a cross check, all three bare cavities have been retested at CERN, in order to cross check their performance, and cross-calibrate the CERN SRF cold test facilities. While achievable transverse deflecting voltage is the key performance indicator, secondary performance aspects derived from multiple cavity monitoring systems are also discussed. Temperature mapping profiles, quench detection, material properties, and trapped magnetic flux effects have been assessed, and the influence on performance discussed. The significant effort invested in developing expertise in preparation and testing of these crab cavities has already been fruitful for all partners, and more is to come within this ongoing program.

INTRODUCTION

As part of the high luminosity upgrade of the Large Hadron Collider (LHC) [1], superconducting compact crab cavities are foreseen for beam crabbing at two of the LHC interaction points. Strong design constraints, in terms both of physical dimension and transverse crabbing voltage have resulted in three innovative designs being taken through to the proof-of-principle stage. These prototypes have been tested in their home labs, and all reached the required specification crabbing voltage of 3.4 MV. In order to gain further experience with these cavity prototypes, and to cross-calibrate the CERN SRF test facility [2] against the home labs of each of the prototypes, a set of vertical cold tests has been carried out, and the results are reported here.

The three crab cavity proof-of-principle designs [3] that have been fabricated and tested are the 4-rod cavity (UK4R) from Lancaster University, the RF Dipole (RFD) from Old Dominion University and the Double Quarter Wave (DQW) cavity from Brookhaven. Figure 1 shows the three prototypes prior to retesting at CERN.

CAVITY PREPARATION

As part of the cold test preparations, two of the cavities (UK4R and DQW) were high pressure rinsed, baked at 120 °C, and then assembled in the SRF ISO4 cleanroom, while the RFD had a similar preparation in its home lab

* karim.gibran.hernandez.chahin@cern.ch

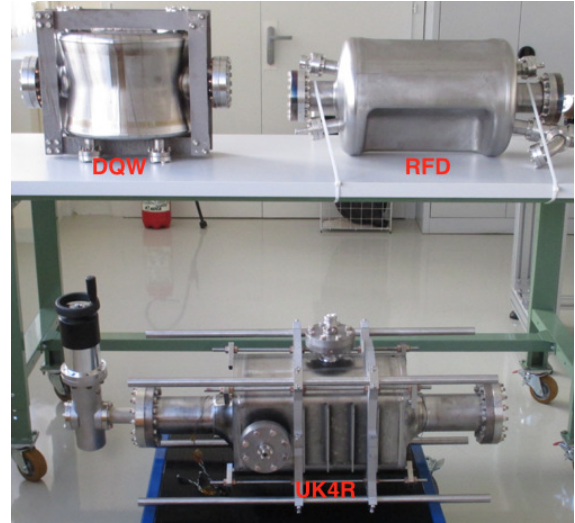


Figure 1: Picture of the crab cavities at CERN.

then shipped under vacuum to CERN. All three cavities were tested in at 2 K in the same 4 m deep cryostat in the CERN SRF facility. Preparation of the RF surface, assembly and installation of the cavity into the cryostat followed the same general steps for all cavities, and are listed below. Prior to the tests reported here, all three cavities previously had a full preparation of the RF surface in their respective home labs.

- BCP, with an average thickness removal of 20 μm
- High Pressure Rinsing, in a 100 bar rinsing cabinet. The rinse is composed of 6 cycles with a di-jet nozzle with vertical nozzle speed of 0.5 mm/s and an angular speed of 3 RPM
- Drying in an ISO4 cleanroom environment with a laminar air flow in the direction along the cavity axis
- Assembly in an ISO4 cleanroom environment
- Mounting on the cryostat insert and leak testing
- Bakeout at 120 °C up to 48 hrs
- Mounting of monitoring and diagnostic equipment, and then installation in the cryostat
- Cool down to 2 K, with the ambient magnetic field suppression.

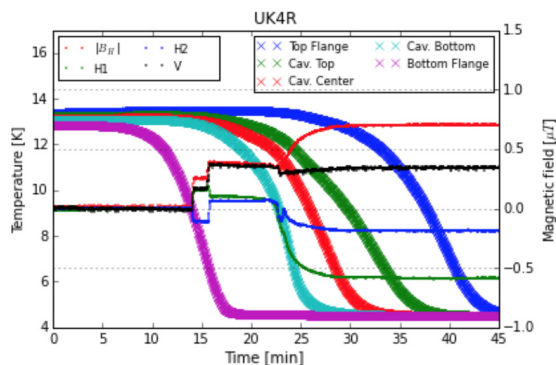


Figure 2: A typical magnetic flux expulsion monitoring during the transition from normal to superconducting, in this case for the UK4R cavity.

Standard monitoring and diagnostic systems [4] deployed on the cryostat insert include quench detector sensors distributed around the cavity, dedicated temperature monitoring using contact temperature sensors (CERNOX, RuO₂, and Allen Bradley resistors), helium level gauges, cavity and helium bath pressure gauges, and single axis magnetic flux probes for residual ambient magnetic field measurement.

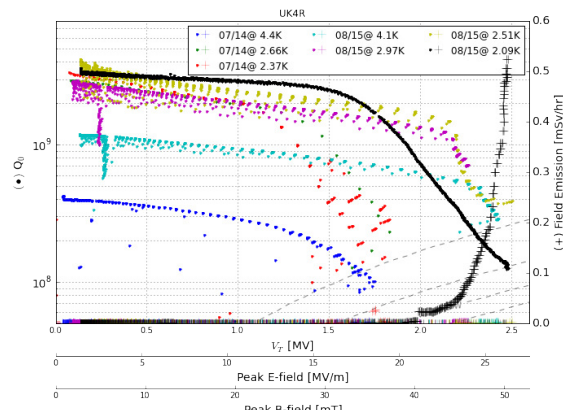
CAVITY PERFORMANCE MEASUREMENTS

Measurement of the three cavity prototypes has been done over the last calendar year, and both expertise and infrastructure evolved and improved over this period [4]. For a summary of the cold testing performed, an overview is given in Table 1.

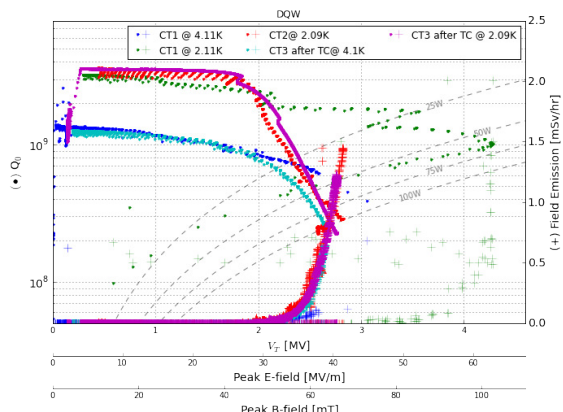
For the ambient magnetic field compensation as listed in Table 1, suppression of the ambient magnetic field prior to the superconducting transition at T_c is done with three independent compensation coils external to the cryostat, which can be used to compensate the magnetic field to a maintainable minimum of 30 nT. Monitoring of the magnetic field components is done by single axis fluxgate monitors mounted 2 cm away from the cavity surface, and compensation can be controlled by a slow feedback loop on the compensation coil power supplies [4]. As a by-product of the magnetic field monitoring, flux expulsion is clearly seen when the cavity passes through the normal-superconducting phase transition, as shown in Fig. 2.

The cool down from 300 K to 4 K is done with a cool down rate of 15 K/min to avoid the onset of Q-disease in the 100 K to 50 K regime. For the transition of the cavity through the superconducting transition at 9.2 K, the standard procedure is to cool down to ~15 K, stop and thermalise, then cool through the transition with a cooling speed of 1 K/min. In this way a controlled spatial thermal gradient and cool down is established.

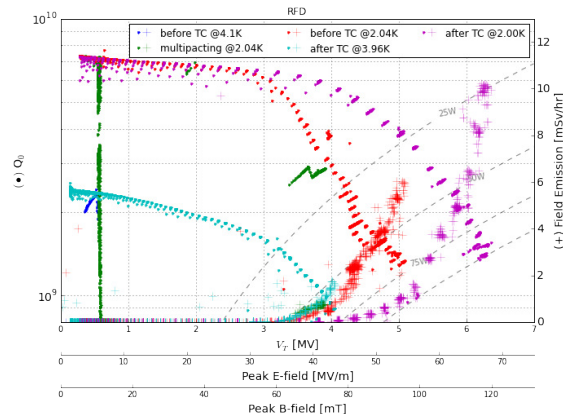
Figure 3 gives a summary of the present the RF performance of each of the cavities during the different cold tests in our test facility. As the RFD was shipped assembled and ready to test, it's cold test offers the best cross check of the



(a) UK4R



(b) DQW



(c) RFD

Figure 3: Q_0 vs V_T for the 3 proof-of-principle crab cavities during the different cold tests.

test stand. Test results achieved at JLab were a low field $Q_0 = 1.25E10$ and $V_{T,Max} = 7MV$ [5]. As can be seen from Fig. 3 we did not quite reach this performance, but the difference was traced to an incomplete magnetic field compensation. (An undetected hardware failure caused the vertical component of ambient magnetic field to be only partially compensated, such that there was a vertical magnetic field component in the order of 3 μT , and this slightly

Table 1: Summary of the Cold Test (CT) Scenarios.

	ColdTest	BCP	HPR	120 °C Bake	Thermal gradient at 9.2 K control at T_c	B field compensation
UK4R	CT 2014	None	LPR	24 Hr	Yes	5 μ T
	CT 2015	Yes	5 Hr	48 Hr	No	5 nT
DQW	CT 2014	40 μ m	1 Hr and Hot N_2	36 Hr	Yes	5 nT
	CT 1 2015	20 μ m	5 Hr	No	No	5 μ T
	CT 2 2015	None	None	36 Hr	No	5 nT
RFD	CT 2014	15 μ m	24 Hr	24 Hr	No	5 μ T

elevated residual resistance, and gave a deterioration of the RF performance. However, the RFD still achieved a $V_{T,Max}$ well above specification, and quenched at high field due to thermal loading in the high E-field region of the cavity, as can be seen by the temperature monitoring shown in Fig. 4, where the sensor T4 shows a steady increase with the field.

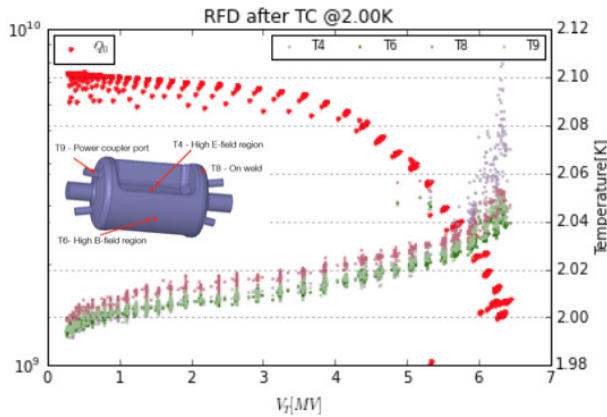


Figure 4: Local heating in the RFD as field is increased.

For the UK4R, performance was limited due to issues with beam port leaks in superfluid helium that prevented a full evaluation of the cavity. The knife edges on the flange have recently been re-machined and the cavity is now leak tight. However, performance is still limited, due to issues with contamination during the high pressure rinse cycle, which was suspected after observing field emission turn on at a mid-field level. After investigation, contamination was traced to a corroding nozzle head on the HPR wand. This, along with the leak on the beam port flange and issues with a stainless steel antenna, has meant $V_{T,Max}$ the performance reach has been limited to close to the specifications value, including an initial test in 2013 [6]. Certainly, the contamination has limited the low-field Q.

Likewise, the DQW cold tests were also plagued by contamination issues, as is evidenced by the early onset of field emission, and the clear Q-switches in Fig. 3. Also, problems with drying the cavity after the HPR were observed, due to the geometry of the design, with residual water collecting in high B-field regions of the RF surface during the normal evaporative drying process. We have since improved our drying process by means of injection of hot nitrogen, but the drying is still under optimisation.

Nevertheless, the DQW $V_{T,Max}$ performance reach, albeit with limited low-field Q, was 4.3 MV in CW operation, which is comparable with the reach obtained by BNL with pulse mode measurements [7]. The cavity is still under test and during the most recent DQW test we were unable to process a mid-field multipactor, as with a fixed input coupler, and an input power limit of 260 W, we could not couple sufficient power into the cavity to process the multipactor. Previously, BNL had processed the multipactor with 200 W input power and a mobile coupler. The DQW will be retested with either a mobile coupler or extended conditioning at 4 K before cooling to 2 K.

LORENTZ FORCE DETUNING

After a refurbishment of our SRF test stand [4], precise resonance frequency tracking is possible, allowing a real time measurement of the Lorentz force detuning. The Lorentz force detuning corresponds to the frequency shift coming from the surface deformation from radiation pressure generated by the electromagnetic field of the cavity; the frequency shift (Δf) proportional to the square of the field V_T^2 . The Lorentz force detuning constant (K_L) is defined by $\Delta f = K_L V_T^2$, and in Fig. 5 the frequency shift data for the DQW is given. A value of $K_{L,DQW} = 259.1 \pm .1 [Hz/MV^2]$ is obtained, with the DQW cavity fixed only at the bottom beam port flange. The measured value is 51Hz above the simulations value (for an unconstrained cavity) [8]. For Fig. 5, changes of the helium bath pressure due to power dissipation in the bath during powering restricts the range of the fit.

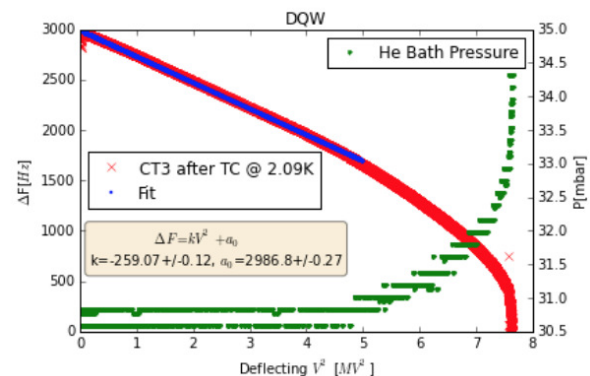


Figure 5: Lorentz force detuning of the DQW.

SURFACE DEFECTS

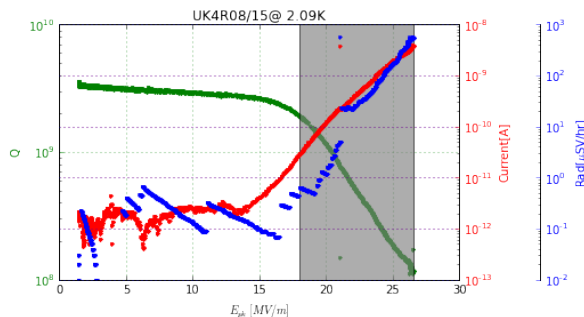
Fowler-Nordheim modelling of field emission current for SRF cavities can be written in terms of the DC dark current measured in the cavity pick-up and the peak electric cavity field. Fowler-Nordheim analysis plots $\ln(I/E^{2.5})$ against $1/E_{\text{peak}}$ and gives the effective area (A_{emitter}) and associated field enhancement factor (β_{FE}) of the emitter [9], where

$$\beta = \frac{B \cdot \phi^{1.5}}{\text{Slope}_{\text{FNS}}} \times 10^{-6},$$

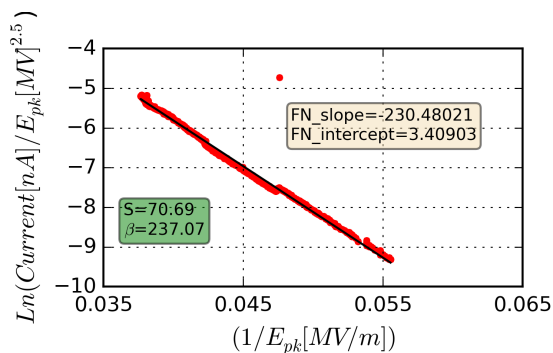
$$A_{\text{emitter}} = \frac{1}{f} \frac{3\pi}{2\sqrt{2}} \frac{1}{AB^2} \frac{(\text{Slope}_{\text{FNS}})^{2.5}}{\phi^2} e^{\text{Intercept}_{\text{FNS}}},$$

with $\phi=4\text{eV}$, $A = 1.54 \times 10^{-6}$ and $B = 6.83 \times 10^9$.

For the 2015 cold tests of the UK4R, significant mid-field field emission was observed, as shown in Fig. 6, and there is a clear correlation between observed radiation immediately outside the cryostat and DC dark current on the cavity pickup antenna. From the associated Fowler-Nordheim analysis given in Fig. 6, the typical effective surface area of the emitter and field enhancement factor are deduced. For the UK4R, the effective surface area of the emitter is $S = 7.1\text{nm}^2$ with a $\beta = 237$. This assumes that the pickup antenna collects all the dark current produced by the emitter, but this is a substantial overestimate. Given that the effective area of the emitter scales inversely to fraction of the dark current it actually observes, one can consider an effective emitter size scaled by at least a factor 100, although this is only a very rough estimate.



(a) UK4R Q₀, DC dark current and radiation vs V_T



(b) UK4R Fowler-Nordheim fit

Figure 6: The region of inters for the Fowler-Nordheim fitting range after the processing at 2K.

MATERIAL PROPERTIES

Material properties for the cavities can be determined by measurement of the frequency change as a function of temperature, with the measurement giving the change in penetration depth, the average electron mean free path and the residual resistance ratio of the RF surface [10]. Unfortunately, as the frequency shift is small, the measurement can be overshadowed by frequency shifts from pressure fluctuations in the cryostat. To avoid this in our cryostat, before warming up the cavity toward T_c , the cryostat is emptied of liquid helium, then pumped down to 30 mbar, so that the influence of pressure fluctuations from the cryogenics system is kept at a minimal. Isothermal heating can then be done and the resonant frequency shift recorded as the cavity warms toward T_c [4], and this measurement was done for the DQW and the UK4R.

Using $\Delta\lambda(T, l) = \frac{G}{\mu_0\pi f^2} \Delta f$ where G is the cavity geometry factor, and $\Delta\lambda(T, l)$ the penetration depth, and the relation $\lambda = \lambda_L \sqrt{1 + \xi_F/l}$ where λ_L is the London penetration depth and ξ_F is the coherent length of the Cooper electrons pair, the electron mean free path l , the penetration depth $\Delta\lambda(T = 0, l)$, mean free path, and RRR can be determined. As shown in Fig. 7, the RRR for the DQW without a 120 °C bake was $RRR_{DQW} = 253.8 \pm 0.1$, and $RRR_{DQW} = 92.5 \pm 0.6$ after a 120 °C bake. This is entirely consistent with the known effect of baking lowering the RRR. The same measurement done for the UK4R after a 120 °C bake gave $RRR_{UK4R} = 10 \pm 0.2$, but the UK4R bakeout was approximately 10 hours longer than that of the DQW.

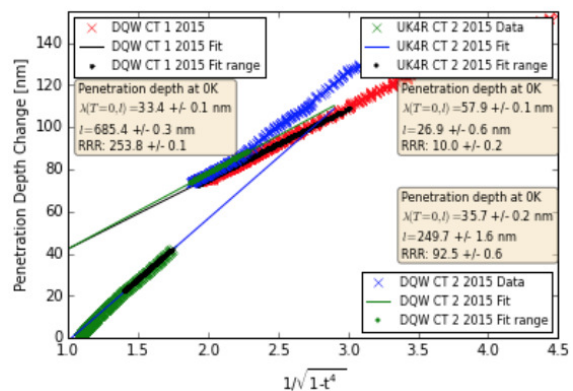


Figure 7: The change in penetration depth as a function of temperature ($t = T/T_c$), with $\lambda(T = 0, l)$ penetration depth, mean free path and RRR extracted for the DQW (baked [CT1] and unbaked [CT2]) and for the baked UK4R.

CONCLUSION

Significant progress has been made in the preparation and test of HL-LHC crab cavities at CERN, with the RF performance approaching the results achieved in other labs. Performance measurements of the RFD, which had surface preparation done in its home lab, showed almost equivalent performance, with only a slight deterioration due to ambient magnetic field that was not fully suppressed. Full

characterisation of the DQW and UK4R cavity prototypes has been limited due to a number of RF surface preparation issues related to the CERN SRF test facility and cleanroom installation. Contamination and drying issues meant that the low-field Q was lower than expected and the transverse deflecting voltage reach was limited by field emission, Q-switches, and high-field multipactors. The source of these problems has been understood, and correction steps are being implemented such that the DQW and UK4R can be retested in clean conditions in the immediate future.

ACKNOWLEDGMENT

The authors would like to acknowledge the technical support and effort from G. Pechaud, M. Gourragne, M. Therasse of the CERN SRF test facility, as well as the cryogenics operations team. Also, this test program would not be possible without the support and cavity prototypes from HL-LHC crab cavities project and we are grateful to the teams from Brookhaven, Lancaster University, Jefferson Lab, and Old Dominion University for sending their cavities to CERN. The research leading to these results has received funding from the European Commission under the FP7 project Hi-Lumi LHC, GA no. 284404, co-funded by the DoE, USA and KEK, Japan, and one of the authors (KH) acknowledges to CONACyT for financial support for this work.

REFERENCES

- [1] P. Baudrenghien, K. Brodzinski, R. Calaga, O. Capatina, E. Jensen, A. Macpherson, E. Montesinos, and V. Parma. Functional specifications of the LHC prototype crab cavity system. In *Internal Note, CERN*, 2013.
- [2] J. Chambrillon, M. Therasse, O. Brunner, P. Maesen, O. Pirotte, B. Vullierme, and W. Weingarten. CERN SRF assembling and test facilities. *Proc. SRF11, Chicago*, 2011.
- [3] R. Calaga. LHC crab cavities, review comments & crab workshop summary. In *Internal Note, CERN*, 2012.
- [4] A. Macpherson, K. Hernandez Chahin, C. Jarrige, P. Maesen, K.-M. Schirm, R. Torres-Sanchez, S. Aull, A. Benoit, P. Fernandez Lopez, R. Valera Teruel, and T. Junginger. Diagnostic Developments at CERN's SRF Testing Facility. In *These proceedings, SRF2015, Whistler, Canada*, 2015.
- [5] S. U. De Silva and J. R. Delayen. Superconducting RF-Dipole deflecting and crabbing cavities. In *Proc. SRF13, Paris*, 2013.
- [6] B. Hall, G. Burt, T. Jones, S. Patalwar, N. Templeton, A.J. May, A.E. Wheelhouse, P.A. McIntosh, R. Calaga, S. Calatroni, E. Jensen, and A. Macpherson. Testing and dressed cavity design for the HL-LHC 4R crab cavity. In *Proc. IPAC1204, Dresden*, 2014.
- [7] Binping Xiao, Luis Alberty, Sergey Belomestnykh, Ilan Ben-Zvi, Rama Calaga, Chris Cullen, Ofelia Capatina, Lee Hammons, Zenghai Li, Carlos Marques, John Skaritka, Silvia Verdu-Andres, and Qiong Wu. Design, prototyping, and testing of a compact superconducting double quarter wave crab cavity. *Physical Review Special Topics - Accelerators and Beams*, 18(4), apr 2015.
- [8] S. Verdu-Andres, B. P. Xiao Q. Wu, S. Belomestnykh, and J. Wang. Lorentz detuning for a double-quarter wave cavity. In *Proc. SRF15, Whistler*, 2015.
- [9] R. H. Fowler and L. Nordheim. Electron Emission in Intense Electric Fields. *Proceedings of the Royal Society A: Mathematical, Physical and Engineering Sciences*, 119(781):173–181, May 1928.
- [10] S. Aull. Derivation of material parameters from cavity cold tests. In *Internal Note, CERN*, 2015.